Mass flow rate correlation for two-phase flow of R218 through a capillary tube

Václav Vinš, Václav Vacek

▶ **To cite this version:**

Václav Vinš, Václav Vacek. Mass flow rate correlation for two-phase flow of R218 through a capillary tube. Applied Thermal Engineering, 2009, 29 (14-15), pp.2816. 10.1016/j.applthermaleng.2009.02.001 . hal-00556848

HAL Id: hal-00556848
https://hal.science/hal-00556848

Submitted on 18 Jan 2011

HAL is a multi-disciplinary open access archive for the deposit and dissemination of scientific research documents, whether they are published or not. The documents may come from teaching and research institutions in France or abroad, or from public or private research centers.

L'archive ouverte pluridisciplinaire **HAL**, est destinée au dépôt et à la diffusion de documents scientifiques de niveau recherche, publiés ou non, émanant des établissements d'enseignement et de recherche français ou étrangers, des laboratoires publics ou privés.

Accepted Manuscript

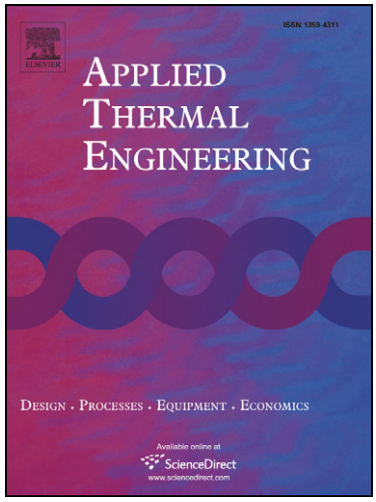

Mass flow rate correlation for two-phase flow of R218 through a capillary tube

Václav Vinš, Václav Vacek

PII: S1359-4311(09)00049-0
DOI: 10.1016/j.applthermaleng.2009.02.001
Reference: ATE 2731

To appear in: *Applied Thermal Engineering*

Received Date: 24 November 2008
Revised Date: 2 February 2009
Accepted Date: 2 February 2009

Please cite this article as: V. Vinš, V. Vacek, Mass flow rate correlation for two-phase flow of R218 through a capillary tube, *Applied Thermal Engineering* (2009), doi: 10.1016/j.applthermaleng.2009.02.001

This is a PDF file of an unedited manuscript that has been accepted for publication. As a service to our customers we are providing this early version of the manuscript. The manuscript will undergo copyediting, typesetting, and review of the resulting proof before it is published in its final form. Please note that during the production process errors may be discovered which could affect the content, and all legal disclaimers that apply to the journal pertain.

ACCEPTED MANUSCRIPT

Mass flow rate correlation for two-phase flow of R218 through a capillary tube

Václav Vinš [a,b,*], Václav Vacek [a]

[a] *Czech Technical University in Prague, Faculty of Mechanical Engineering, Technická 4, 16607 Prague 6, Czech Rep.*

[b] *Institute of Thermomechanics AS ČR, v.v.i., Dolejškova 1402, 18200 Prague 8, Czech Rep.*

Abstract

This paper presents some experimental results of refrigerant two-phase flow through a capillary tube. The data was obtained for fluorinert refrigerant R218, which is used in some special vapor cooling circuits, e.g. in various particle detectors at the CERN international research centre. An analytical correlation for mass flow rate of R218 was prepared on the bases of dimensionless parameters derived from the Buckingham π-theorem. Two approaches were compared: (a) the conventional power law function and (b) correlation determined with the use of an artificial neural network. Measured data were also correlated with other mass flow rate correlations presented in literature.

Keywords: Artificial neural network; Capillary tube; Mass flow rate correlation; R218

* Corresponding author. Tel: +420 608 514 106; fax: +420 286 584 695.

E-mail address: vins.vaclav@seznam.cz (V. Vinš)

ACCEPTED MANUSCRIPT

ACCEPTED MANUSCRIPT

Nomenclature

a	neuron output
A	capillary tube cross section, [m^2]
AD	average deviation, [%]
c_p	specific heat, [$J \cdot kg^{-1} \cdot K^{-1}$]
d	capillary tube inner diameter, [m]
h	enthalpy, [$J \cdot kg^{-1}$]
Ib	bias in input layer
IW	weight coefficient in input layer
k	number of data points
L	capillary tube length, [m]
Lb	bias in output layer
LW	weight coefficient in output layer
$\dot{m}$	mass flow [$kg \cdot s^{-1}$]
n	net input
p	absolute pressure, [Pa]
P	power law coefficient
Re	Reynolds number
SD	standard deviation, [%]
T	temperature, [K]

Greek letters

ε	wall roughness, [m]
μ	viscosity, [Pa·s]
π	dimensionless parameter
ρ	density, [$kg \cdot m^{-3}$]
σ	surface tension, [$N \cdot m^{-1}$]

Subscripts

cor	correlated data
crit	condition at critical point
exp	experimental data
evap	evaporative
i	input index
in	condition at capillary tube inlet
j	neuron index
L	liquid phase
sat	condition at liquid saturation curve
sub	subcooling
tube	connecting tube
V	vapor phase

Superscripts

–	normalized parameter within (-1,1)
′	weighted parameter

ACCEPTED MANUSCRIPT

1. Introduction

Small bore tubes, known as capillary tubes, are used as expansion devices in some vapor cooling circuits. They are commonly installed in small cooling systems such as household refrigerators and air conditioning systems due to their low cost and simple design. Capillary tubes can also be useful for certain special applications, namely in situations where the compressor-condenser unit is located far away from the evaporator and it would not be possible to use a thermostatic valve due to space limitations and environmental constraints. The design of such cooling systems for the ATLAS [1] and TOTEM [2, 3] experiments at CERN required a detailed study of the capillary flow using fluorinert refrigerant R218 (C_3F_8, octafluoropropane). In spite of its relatively poor thermodynamic performance, R218 is used for cooling particle detectors or microelectronics, as it is radiation resistant, chemically stable and as it has outstanding dielectric properties.

Though the capillary tube seems to be quite a simple device, its proper design for a cooling circuit is quite complex. Many studies have investigated two-phase capillary flow in the last 50 years. Some of them have used mathematical approaches based on numerical simulations to generate a theoretical model of capillary flow. Most of these models have considered two thermodynamic equilibrium regions of subcooled liquid and a two-phase vapor-liquid mixture [4, 5, 6, 7]. The two-phase flow has been generally simplified as a homogeneous flow with the same velocities of both phases. Another approach, employed for instance by Seixlack and Barbazelli [8], is based on a two-fluid model when the hydrodynamic and thermodynamic non-equilibrium between liquid and vapor phases is considered. The most accurate simulations including the

ACCEPTED MANUSCRIPT

metastable region of capillary flow were prepared by Guobing and Yufeng [9], Wongwises et al. [10] and García-Valladares et al. [11, 12, 13, 14].

Other researchers have measured capillary flow experimentally, using capillary tubes with temperature and pressure sensors placed along their length [15, 16, 17, 18, 19]. The data provided by these authors has contributed to a better understanding of capillary flow behavior. The metastable flow phenomenon was experimentally investigated in detail and afterwards mathematically modeled, for instance by Li et al. [20] for adiabatic flow of R12 and by Chen et al. [21] for non-adiabatic flow of R134a.

Melo et al. [22], Kim et al. [23], Choi et al. [24, 25] and Jabaraj et al. [26] tested a set of capillary tubes with different inner diameters and lengths under varying inlet and outlet conditions. The significant amount of collected data enabled the authors to develop analytical correlations for the mass flow rate. The standard power law function was applied to the dimensionless parameters obtained from the Buckingham π-theorem [27]. These correlations provide good results and can therefore be used for a quick initial capillary tube design. A limitation of these correlations lies in fact that they can be properly used only in the range of measured capillary flow conditions and for conventional refrigerants such as R12, R22, R134a, R600a and refrigerant mixtures R407C, R410A, R407C/R600a/R290.

Zhang [28] introduced a different method for determining the mass flow rate correlation based on an artificial neural network (ANN), using experimental data from the literature. His correlation provides more precise results than power law functions. Zhang et al. presented a more general mass flow rate correlation in a second paper [29]. Neural network training and testing were based both on experimental data from others and on theoretical data simulated by using a homogeneous equilibrium model similar to

ACCEPTED MANUSCRIPT

Sami and Tribes [5] or Kritsadathikarn et al. [6]. An ANN correlation can be used for predicting refrigerant mass flow for both subcooled and two-phase inlet conditions. Nevertheless, the correlation generated in this way is rather complicated, as it uses six neurons in a hidden layer. Islamoglu et al. [30] introduced another ANN model of refrigerant flow through a non-adiabatic capillary tube placed inside a suction heat exchanger.

A detailed review of the most relevant studies based both on the experimental tests and the theoretical modeling of the capillary flow has been recently presented by Kumar et al. [31].

2. Aim for this study

The first objective of our study was to get new experimental data for the capillary flow of fluorinert refrigerant R218, since the most comparisons in the literature use repeatedly the same source of experimental data measured either with environmentally inconvenient refrigerants R12 and R22 or with their alternatives R134a, R407C or R410A. The second aim of the study was to derive an analytical correlation for the mass flow rate of R218 through an adiabatic capillary tube. Two approaches based on the dimensional analysis were employed: the power law function and the ANN. Our experimental capillary flow data were measured in an oil-less cooling circuit and with refrigerant exempt of non-condensing gases; therefore the refrigerant is not contaminated, as seems to be the case in several relevant studies presented in the literature (either by the presence oil fractions or non-condensing gases).

ACCEPTED MANUSCRIPT

3. Experimental set up

Refrigerant flow through a set of copper and copper-nickel capillary tubes was measured inside the vapor cooling circuit shown in Fig. 1. The cooling circuit used a combination of two oil-free compressors; a membrane unit increased the pressure by 2 bars and a piston unit by 15 bars. The whole system was versatile and allowed all operating conditions of the capillary flow to be varied: the inlet pressure was controlled and set by a regulating valve; the inlet temperature could be varied either by a subcooling unit consisting of a secondary capillary tube and a counter-flow heat exchanger (HEX) or by a heater placed before the inlet to the tested capillary tubes. The evaporator was realized as a PID-controlled heater with set point at about + 26 °C. The evaporative pressure was set by a backpressure regulator (BPR). The subcooled liquid pressure could be increased by a magnetic pump placed between two heat exchangers using chilled water.

The parameters of the refrigerant flow through the circuit were monitored by a set of calibrated temperature sensors with an uncertainty ± 0.1 °C in considered temperature range and by precise absolute pressure gauges. Pressure transducers used at the liquid line had range 0 ÷ 30 bar with an uncertainty ± 0.033 % of full scale. Units installed at the vapor line had lower range of 0 ÷ 5 bar and an uncertainty ± 0.2 % of full scale. The refrigerant mass flow rate – the main measured parameter – was monitored by several different flow meters. A precise Coriolis mass flow meter type with uncertainty 0.5 % of reading and a turbine volumetric flow meter type with an uncertainty 1 % of reading were installed in the high pressure liquid line. A thermal flow sensor type and a volumetric flow meter type both with an uncertainty 2 % of reading were installed in the low pressure vapor line. The output signals of all the

ACCEPTED MANUSCRIPT

sensors were read by a mobile DAQ system based on an Embedded Local Monitor Board (ELMB) device [32], a Kvaser[1] CANbus card and a notebook with PVSS II[2] software.

4. Methodology and experimental results

Each of the tested capillary tubes was carefully prepared before being installed in the cooling circuit. The length of all capillary tubes was measured with an uncertainty ± 0.3 mm. The wall roughness was measured using a roughness measuring instrument 'MarSurf PS1'[3]. A sample of each capillary tube was cut using a precise grinding machine and afterwards cleaned in an ultrasound bath. The relative wall roughness ε/d was analyzed in a similar way as suggested by Brackbill et al. [33]. Two methods, optical and weighing, were used to determine the inner diameter – the dominant parameter affecting the overall capillary tube performance. Similarly to Mikol [15] and Li et al. [17], both methods gave comparable results with a difference below 4 %. The optical method was more time consuming due to the sample preparation. Since the number of capillary tubes to measure was relatively large, the repeated weighting method was mainly employed. The average inner diameter was calculated from a comparison of the weight of an empty and filled capillary tube with available fluorinert. An accurate scale with precision of 0.001 g was used for this purpose. Fluorinert liquid C_7F_{16}, having approximately 1.7 x higher density than water under standard laboratory conditions, was used as the filling liquid. The inner diameter was determined with an uncertainty ± 0.003 mm for small diameter capillary tubes ($d \sim 0.5$ mm) and

[1] Kvaser AB, Aminogatan 25 A, SE 431 53 Mölndal, Sweden; http://www.kvaser.com/
[2] ETM professional control GmbH, A Siemens Company, Kasernenstraße 29, A-7000 Eisenstadt, Austria; http://www.etm.at/
[3] Mahr GmbH, Carl-Mahr-Str.1, D-37073 Göttingen, Germany; http://www.mahr.de/

ACCEPTED MANUSCRIPT

± 0.001 mm for larger capillary tubes (d ~ 1.0 mm). The capillary tubes were cleaned using C_7F_{16}, as fluorinert liquids have a slight solvent behavior. The cuts at the capillary tube ends were treated carefully in order to prevent dirt or a squeezed capillary inner diameter which might significantly affect the refrigerant flow. The capillary tube edges were cleaned with a small precision drill before installation into the circuit. 'Armaflex'[4] insulation was used to insulate all the capillary tubes, securing them under adiabatic flow conditions. A list of the tested capillary tubes together with ranges of the main refrigerant flow conditions are shown in Table 1.

Some of the investigated capillary tubes were equipped with temperature sensors installed along the length. 'Kapton' coated type NTC temperature sensors were attached to the outer surface of the capillary tubes using a thermal glue paste and a metal tape. The temperature variation detected along the capillary tubes provided useful information on refrigerant flow status. Fig. 2 shows the pressure and the saturation pressure curves for an adiabatic capillary tube including the metastable flow region. The saturation pressure calculated from the measured temperature and the relevant thermophysical properties of R218 is compared with the measured absolute pressure at the capillary tube inlet and outlet, and with the theoretical pressure development predicted via numerical simulation presented by Vacek and Vinš [34]. The metastable region is a thermodynamically non-equilibrium phenomenon in which single-phase liquid flow remains at a pressure lower than saturation pressure. According to the results obtained from the numerical simulation, the saturation pressure should start to drop already at a distance around 0.9 m from the inlet. However, the experimentally

[4] Armacell LLC, 7600 Oakwood Street Ext., Mebane, NC 27302; http://www.armacell.com/

ACCEPTED MANUSCRIPT

measured temperature remained constant a little longer indicating the existence of the metastable flow.

5. Mass flow correlation based on the power law function

A total of 189 data points fulfilling the adiabatic choked flow condition of R218 flow through a capillary tube were collected during the test and analyzed to determine the analytical mass flow correlation.

Dimensional analyses of adiabatic capillary flow under choked flow conditions have been presented in detail in the literature [22, 23, 24, 25]. The determination of the dimensionless parameters is therefore not presented in detail in this paper. Table 2 summarizes the most common dimensionless parameters together with an explanation used for the description of the adiabatic capillary flow. The simple, precise and reliable form of dimensionless parameters from π_1 to π_8 introduced by Choi et al. [24] was selected for our study.

In Table 2, refrigerant properties such as densities, viscosities and surface tension are considered as functions of the inlet temperature. All these thermophysical properties were obtained using the REFPROP database [35] with provisional data files, and were correlated with previously published measurements realized with fluorinerts and mixtures of fluorinerts [36, 37]. The refrigerant mass flow rate can be derived directly from parameter π_8, which is defined in standard power law form, Eq. (1). Coefficients were evaluated from our data using a non-linear regression technique.

$$\pi_8 = 7.43 \cdot 10^{-3} \pi_1^{0.22059} \pi_2^{-0.04803} \pi_3^{-0.51390} \pi_4^{-3.01166} \pi_5^{1.04197} \pi_6^{-0.13653} \pi_7^{2.24975} \quad (1)$$

ACCEPTED MANUSCRIPT

The relative deviation of the correlated mass flow rate from the experimental data, defined as $(\dot{m}_{exp} - \dot{m}_{cor}) / \dot{m}_{exp} 100$, is shown in Fig. 3. The average and standard deviations of the correlated data,

$$AD = \frac{1}{k} \sum_{k} \left(\dot{m}_{exp} - \dot{m}_{cor} \right) / \dot{m}_{exp} 100 \tag{2}$$

$$SD = \sqrt{\frac{1}{k} \sum_{k} \left[\left(\dot{m}_{exp} - \dot{m}_{cor} \right) / \dot{m}_{exp} 100 \right]^2 - AD^2} \tag{3}$$

are - 0.41 % and 4.85 % respectively. 162 data points lie in the range of relative deviation ± 7 %; this is equal to 85.7 % of the experimental data. Most of the data outside this deviation range corresponds to refrigerant flow through small diameter capillary tubes with the mass flow rate under 0.75 $g \cdot s^{-1}$.

6. Artificial neural network correlation

The mass flow rate correlation based on the power law function approximates the experimental data relatively well. However, there are still some limitations of such a simple function. As cited by Zhang [28], the main problem lies in the fact that the power law function collapses and provides abnormal results in the case of zero subcooling. Another complication shown in the previous section can occur when predicting low mass flow rates inside small diameter capillary tubes.

The complex mechanism of the flow through a capillary tube is a non-linear multi-input and single-output problem, which can be solved for instance by the ANN. MATLAB software [38] especially the 'Neural Network Toolbox' was used in this study, instead of generating our own code.

A three layer perceptron, consisting of an input, one hidden and one output layer, was employed for the mass flow rate correlation. As in the case of the power law

ACCEPTED MANUSCRIPT

correlation function, parameters π_1 to π_7 are considered as inputs, and parameter π_8 is solved as a single-output. Four configurations of the three-layer perceptron with different numbers of neurons in the hidden layer were tested. The scheme of the three-layer perceptron with two neurons in the hidden layer is shown in Fig. 4.

The inputs, in our case dimensionless parameters π_1 to π_7, are transmitted through a connection that multiplies their strength by scalar weights, $\pi_i' = IW_{i,j}\pi_i$; index *i* marks a certain input parameter, index *j* states the neuron inside the hidden layer. As is shown in Fig. 4, the neuron consists of a summation function and a transfer function. The result of the summation function, net input n_i, is given as the sum of the weighted inputs and the input bias, $\sum \pi_i' + Ib_i$. In the ANN presented here, the transfer function is considered as a sigmoid function, Eq. (4).

$$a_j(n_j) = 1/(1+e^{-n_j}) \tag{4}$$

The output layer uses a standard linear function; the output π_8 is estimated as the sum of the weighted results of the hidden layer and the output layer bias, $\pi_8 = \sum LW_j a_j + Lb$.

An important part of an ANN algorithm is the training step, when the connection weights are found for a given set of proper inputs and outputs. In this study, the 'batch gradient descent with momentum' back propagation learning algorithm was employed. This method has several significant advantages, such as fast convergence, the network responds to trends in the error surface and hence should not be sensitive to local minima in the error surface.

Due to the character of the sigmoid transfer function, it is suggested that the inputs should lie within (-1, 1) or the ANN would not work properly. The MATLAB

ACCEPTED MANUSCRIPT

normalization function 'premnmx' is applied to all inputs before the back propagation learning algorithm starts. The normalized π-parameter is defined as:

$$\bar{\pi} = 2\left[\pi - min(\pi)\right] / \left[max(\pi) - min(\pi)\right] - 1 \tag{5}$$

Output parameter π_8 should be denormalized after the ANN algorithm by using MATLAB function 'postmnmx' to obtain its real value. Denormalized π_8 is determined from Eq. (6).

$$\pi_8 = 0.5\left(\bar{\pi}_8 + 1\right)\left[max(\pi_8) - min(\pi_8)\right] + min(\pi_8) \tag{6}$$

Table 3 sums up the minimum and maximum values of all inputs, π_1 to π_7, and target output π_8. These values serve to preprocess the inputs and postprocess the output, using the described relations (5) and (6), whenever the presented network is used.

Four configurations of the three-layer perceptron with varying number of neurons in the hidden layer were tested in this study. The mass flow rate correlation obtained from ANN with one neuron in the hidden layer has certain problems with convergence, and does not provide good results. Only 73.5 % of the experimental data is correlated within the range of relative deviation ± 7 %, which is worse than the results obtained from the power law function. Cases with two and more neurons in the hidden layer have practically the same accuracy. The average deviation and standard deviations are approximately 0.1 % and 3.4 % respectively. A configuration with two neurons in the hidden layer was chosen as a suitable ANN correlation for refrigerant mass flow rate.

Normalized output parameter $\bar{\pi}_8$, for ANN correlation with two neurons in the hidden layer, is determined from Eq. (7).

$$\bar{\pi}_8 = -3.8314 \frac{1}{1+e^{-n_1}} + 0.7616 \frac{1}{1+e^{-n_2}} + 2.3454 \tag{7}$$

The net inputs n_1 and n_2 are defined as:

ACCEPTED MANUSCRIPT

$$
\begin{aligned}
n_1 &= -0.7302\bar{\pi}_1 + 0.6391\bar{\pi}_2 + 2.7096\bar{\pi}_3 - 0.8606\bar{\pi}_4 - \\
&\quad -1.5090\bar{\pi}_5 + 0.4891\bar{\pi}_6 + 1.7863\bar{\pi}_7 + 3.1110 \\
n_2 &= 1.8292\bar{\pi}_1 - 0.0923\bar{\pi}_2 - 0.5601\bar{\pi}_3 + 0.5757\bar{\pi}_4 - \\
&\quad -0.8142\bar{\pi}_5 - 0.1093\bar{\pi}_6 + 1.9574\bar{\pi}_7 + 3.6118
\end{aligned}
\tag{8}
$$

Form of the ANN correlation (7) corresponding to two neurons in the hidden layer is quite simple. However in case of the network with more neurons, the mass flow rate correlation becomes quite complicated and inconvenient for practical use. The ANN could be then replaced for instance by the approach introduced by Ponton and Klemeš [39].

A comparison of the experimentally measured mass flow rate with the correlated data using the ANN correlation (7) is shown in Fig. 5. Unlike the case of the power law correlation, problems with the low mass flow rate in small diameter capillary tubes have been solved, see Fig. 3.

An example of experimental data measured on one copper-nickel capillary tube is shown in Fig. 6. The only variable causing mass flow rate variation was the temperature of the subcooled liquid phase, as the absolute pressure at the capillary tube inlet was constant at 14.1 bar. The experimental data are compared with power law and ANN correlations. The power law correlation predicts a higher mass flow rate than experimentally measured. The largest difference was observed at high levels of subcooling typical of the long single-phase flow region and the short two-phase flow region with a sharp pressure drop. The ANN correlation provides better agreement with the experiment than the power law correlation. Only in the case of warm liquid refrigerant does the correlation predict slightly higher mass flow rate than the experimental measurement.

ACCEPTED MANUSCRIPT

7. Comparison of other mass flow rate correlations

Many researchers introduced the refrigerant mass flow rate correlation based on analysis of both their own experimental data and the data presented in literature. We summarize some of these correlations and compare their accuracy on the selection of experimental data available in the open literature. All investigated correlations were also tested on our experimental data measured with R218. The list of considered dimensionless parameters can be found in Table 2.

Melo's [22] correlation was taken in account in our study at first, as it is based on regression of a very large amount of experimental data exceeding 1000 data points. The data were measured inside eight different capillary tubes with refrigerants R12, R134a and R600a. Even though the generated mass flow rate correlation (9) can be found, being relatively simple it provides quite accurate results over a wide range of operating conditions.

$$\pi_9 = 0.195\pi_{10}^{0.448}\pi_3^{-0.528}\pi_{11}^{0.164} \tag{9}$$

Another quite reliable correlation was introduced in the ASHRAE handbook [40]. Compared to Melo, the ASHRAE correlation also considers the influences of friction, density variation and vaporization. The parameters were determined from regression of experimental data measured with refrigerants R134a, R22 and R410A.

$$\pi_9 = 1.8925\pi_{10}^{1.369}\pi_3^{-0.484}\pi_{11}^{0.0187}\pi_{12}^{-0.824}\pi_4^{0.773}\pi_5^{0.265} \tag{10}$$

Kim et al. [23] generated a similar correlation to that presented in the ASHRAE handbook. The correlation additionally takes into account the effect of vapor bubble growth. The authors measured the mass flow rate of R22 and its alternatives R407C and R410A in straight and coiled capillary tubes. Basic form of the correlation applicable for straight tubes is defined by Eq. (11).

ACCEPTED MANUSCRIPT

$$\pi_9 = 1.5104\pi_{10}^{0.5351}\pi_3^{-0.3785}\pi_{11}^{0.1074}\pi_{12}^{-0.1596}\pi_{13}^{0.096} \quad (11)$$

Choi et al. [24] recently experimentally investigated the mass flow rate through straight capillary tubes under adiabatic flow conditions. A generalized correlation was developed for the calculation of the mass flow rate of alternative refrigerants of R12 and R22 on the basis of experimental data measured with R22, R290 and R407C. The set of dimensional parameters has a complex form and describes quite accurately the capillary flow behavior including all main flow effects.

$$\pi_8 = 1.313\cdot 10^{-3}\pi_1^{-0.087}\pi_2^{0.188}\pi_3^{-0.412}\pi_4^{-0.834}\pi_5^{0.199}\pi_6^{-0.368}\pi_7^{0.992} \quad (12)$$

In another work of Choi et al. [25], a general mass flow rate correlation, quite similar to Eq. (12), was presented. The correlation parameters were derived from regression of wide set of literature data for refrigerants R12, R22, R134a, R152a, R407C and R410A.

$$\pi_8 = 0.5782\cdot 10^{-4}\pi_1^{-0.315}\pi_2^{0.369}\pi_3^{-0.344}\pi_4^{0.034}\pi_5^{0.040}\pi_6^{-0.458}\pi_7^{0.376} \quad (13)$$

One of the latest correlations of the mass flow rate through adiabatic straight capillary tubes was generated by Zhang [28]. The author summarized the majority of the data presented in literature and used a more global approach for the correlation estimation than a simple power law function.

$$\pi_8 = 1\Big/\left[1+\exp\left(2.956h-0.064\right)\right]$$
$$h = 1\Big/\left[1+\exp\begin{pmatrix}0.654-5.371\pi_1+7.332\pi_2-9.541\cdot 10^{-4}\pi_3-0.1588\pi_4\\ +2.277\cdot 10^{-2}\pi_5-5.202\cdot 10^{4}\pi_6+1.731\cdot 10^{-2}\pi_7\end{pmatrix}\right] \quad (14)$$

Table 4 summarizes average *AD* and standard *SD* deviations for six investigated correlations presented in literature. The correlations were compared with both the experimental data presented in the literature for pure refrigerants (R12, R22, R134a, R290 and R600a) and with our experimental data measured for R218. The data taken

ACCEPTED MANUSCRIPT

from other researchers was considered having comparable accuracy, i.e. none data set was favored during *AD* and *SD* evaluation. Bold marked results in Table 4 were found as the most accurate. It was observed during investigation of the mass flow rate correlations presented in the literature, that the accuracy of the correlations for one particular refrigerant varies quite significantly for data sets introduced by different researchers. For instance the average deviation of Choi's correlation (12) from the R22 data presented by Chang and Ro [18] is - 5.0 % while from the data introduced by Kuehl and Goldschmidt [41] it is already 18 % by approximately the same standard deviation equal to 1.0 %. This is mainly caused by the correlations' coefficients having been evaluated from data lying in a certain range of operating conditions. Application of the correlations out of the range of experimental conditions, e.g. p_{in}, T_{in}, d, can lead to a significant difference of the predicted data. In all the considered correlations the effects of oil or non-condensing gases present inside the cooling circuit were neglected. In the course of our present experiments, significant evidence of the influence of non-condensing gases (mostly air and nitrogen in our applications) on the capillary tube performance was detected.

The majority of data taken from the open literature were those of Melo [22]. Therefore Melo's correlation (9) shows the best agreement with the experimental data of R12, R134a, and R600a. Choi's correlation (12) provides the best results for R290, as it was also fitted directly to a considered data set. The R22 capillary flow was correlated most accurately by ASHRAE (10) and again by Melo's (9) correlations. Zhang's (14) correlation could be also successfully used for mass flow rate estimation. The worse overall results were obtained from Kim's correlation (11), which has good accuracy only for R22.

ACCEPTED MANUSCRIPT

All correlations were also tested on two sets of our experimental data measured with R218. The first set of 189 data points ('fitted data') was used for generation of our power law and ANN mass flow rate correlations. The second set of 34 data points ('test data'), measured on three copper-nickel capillary tubes with inner diameter of 0.95 mm and lengths of 5.95 m, 3.93 m and 2.38 m, served just for testing the correlations. Comparison of the literature correlations with the experimental data of R218 shows that none of six tested correlations could be in general used for sufficient mass flow rate prediction.

The ANN correlation is in quite good agreement with considered experimental data of the standard refrigerants presented in the literature. The only problem occurred by set of experimental data with R22. The ANN predicts in some cases even better mass flow rate than the general correlations of Choi (13) and Zhang (14). It can be therefore applied not only for particular mass flow rate estimation of R218 but also for a rough prediction for other standard refrigerants.

8. Summary

An experimental study was performed of R218 flow through copper and copper-nickel capillary tubes with different inner diameters and lengths. A comparison of the measured temperature development over the capillary tube with theoretical numerical simulation pointed to the existence of a metastable flow region. The collected data served to determine two mass flow rate correlations of R218 flow through an adiabatic capillary tube: one based on the classical power law function, and one determined using the ANN. The average and standard deviations of the correlated data with the power law function are - 0.41 % and 4.85 % respectively. The ANN correlation with two neurons

ACCEPTED MANUSCRIPT

in the hidden layer is more precise with the average and the standard deviation - 0.12 % and 3.45 %. It is recommended that the mass flow rate correlations presented here be used within the range of operating conditions listed in Table 1; in other cases further validation should be made.

Mass flow rate correlations available in literature were tested both with the standard refrigerants data presented in literature and with our data measured on R218. The comparison showed that none of the considered literature correlations can be sufficiently applied on R218 capillary flow prediction. Moreover it was demonstrated, that presented ANN correlation can be used for primary approximate estimation of mass flow rate also for other refrigerants than R218.

ACCEPTED MANUSCRIPT

ACCEPTED MANUSCRIPT

Acknowledgements

The authors are grateful to ATLAS and TOTEM teams at CERN laboratory for their support during the experimental test on the local cooling circuit. This project was partly supported by grants of the Ministry of Education, Youth and Sports of the Czech Republic LA08015, LA08032, by research program MSM 6840770035 and by research plan of the Institute of Thermomechanics AS ČR, v.v.i. AV0Z20760514.

References

[1] M. Olcese, S.J. Haywood, L.P. Rossi, S.J. McMahon, V. Vacek, R.L. Bates, P. Bonneau, M. Doubrava, M. Battistin, S. Berry, H. Pernegger et al., The evaporative cooling system for the ATLAS Inner detector, Journal of Instrumentation 3 (2008) doi: 10.1088/1748-0221/3/07/P07003.

[2] M. Oriunno, M. Battistin, E. David, P. Guglielmini, C. Joram, E. Radermacher, G. Ruggiero, V. Vacek, V. Vins, J.H. Wu, Design and prototype studies of the TOTEM Roman pot detectors, Nuclear Instruments and Methods in Physics Research A 581 (2007) 499-503.

[3] M. Deile, E. Radermacher, M. Oriunno, G. Ruggiero, V. Vacek, V. Vins et al., The TOTEM experiment and the CERN Large Hadron Collider, Journal of Instrumentation 3 (2008) doi: 10.1088/1748-0221/3/08/S08007.

[4] P.K. Bansal, A.S. Rupasinghe, An homogeneous model for adiabatic capillary tubes, Applied Thermal Engineering 18 (1998) 207-219.

ACCEPTED MANUSCRIPT

[5] S. M. Sami, C. Tribes, Numerical prediction of capillary tube behaviour with pure and binary alternative refrigerants, Applied Thermal Engineering 18 (1998) 491-502.

[6] P. Kritsadathikarn, T. Songnetichaovalit, N. Lokathada, Pressure Distribution of Refrigerant Flow in an Adiabatic Capillary Tube, Research Article, Science Asia 28 (2002) 71-76.

[7] M. Fatouh, Theoretical investigation of adiabatic capillary tubes working with propane/n-butane/iso-butane blends, Energy Conversion and Management 48 (2007) 1338-1348.

[8] A.L. Seixlack, M.R. Barbazelli, Numerical analysis of refrigerant flow along non-adiabatic capillary tubes using a two-fluid model, Applied Thermal Engineering 29 (2009) 523-531.

[9] Z. Guobing, Z. Yufeng, Numerical and experimental investigations on the performance of coiled adiabatic capillary tubes, Applied Thermal Engineering 26 (2006) 1106-1114.

[10] S. Wongwises, M. Suchatawut, A simulation for predicting the refrigerant flow characteristics including metastable region in adiabatic capillary tube, International Journal of Energy Research 27 (2003) 93-109.

[11] O. García-Valladares, C.D. Pérez-Segarra, A. Oliva, Numerical simulation of capillary tube expansion devices behavior with pure and mixed refrigerants considering meta-stable region, Applied Thermal Engineering 22 (2002) 173-182.

ACCEPTED MANUSCRIPT

[12] O. García-Valladares, Numerical simulation of non-adiabatic capillary tubes considering metastable region. Part I: Mathematical formulation and numerical model, International Journal of Refrigeration 30 (2007) 642-653.

[13] O. García-Valladares, Numerical simulation of non-adiabatic capillary tubes considering metastable region. Part II: Experimental validation, International Journal of Refrigeration 30 (2007) 654-663.

[14] O. García-Valladares, Numerical simulation and experimental validation of coiled adiabatic capillary tubes, Applied Thermal Engineering 27 (2007) 1062-1071.

[15] E.P. Mikol, Adiabatic single and two phase flow in small bore tubes, ASHRAE Journal (1963) 75-86.

[16] H. Koizumi, K. Yokoyama, Characteristics of refrigerant flow in a capillary tube, ASHRAE Transactions 86 (1980) 19-27.

[17] R.Y. Li, S. Lin, Z.Y. Chen, Z.H. Chen, Metastable flow of R12 through capillary tubes, International Journal of Refrigeration 13 (1990) 181-186.

[18] S. Chang, S. Ro, Experimental and numerical studies on adiabatic flow of HFC mixtures in capillary tubes, Proceedings of the International Refrigeration Conference at Purdue 1996, Purdue University, USA, 83-88.

[19] A.A.S. Huerta, F.A.S. Fiorelli, O.M. Silvares, Metastable flow in capillary tubes: An experimental evaluation, Experimental Thermal and Fluid Science 31 (2007) 957-966.

[20] R.Y. Li, S. Lin, Z.H. Chen, Numerical modeling of thermodynamic non-equilibrium flow of refrigerant through capillary tubes. ASHRAE Transactions 96 (1990) 542-549.

ACCEPTED MANUSCRIPT

[21] D. Chen, S. Lin, Underpressure of vaporization of refrigerant R-134a through a diabatic capillary tube, International Journal of Refrigeration 24 (2001) 261-271.

[22] C. Melo, R.T.S. Ferreira, C.B. Neto, J.M. Goncalves, M.M. Mezavila, An experimental analysis of adiabatic capillary tubes, Applied Thermal Engineering 19 (1999) 669-684.

[23] S.G. Kim, M.S. Kim, S.T. Ro, Experimental investigation of the performance of R22, R407C and R410A in several capillary tubes for air-conditioners. International Journal of Refrigeration 25 (2002) 521-531.

[24] J. Choi, Y. Kim, H.Y. Kim, A generalized correlation for refrigerant mass flow rate through adiabatic capillary tubes, International Journal of Refrigeration 26 (2003) 881-888.

[25] J. Choi, Y. Kim, J.T. Chung, An empirical correlation and rating charts for the performance of adiabatic capillary tubes with alternative refrigerants, Applied Thermal Engineering 24 (2004) 29-41.

[26] D.B. Jabaraj, A.V. Kathirvel, D.M. Lal, Flow characteristics of HFC407C/HC600a/ HC290 refrigerant mixture in adiabatic capillary tubes, Applied Thermal Engineering 26 (2006) 1621-1628.

[27] E. Buckingham, On Physically Similar Systems; Illustrations of the Use of Dimensional Equations, Physical Review 4 (1914) 345-376.

[28] C.L. Zhang, Generalized correlation of refrigerant mass flow rate through adiabatic capillary tubes using artificial neural network, International Journal of Refrigeration 28 (2005) 506-514.

ACCEPTED MANUSCRIPT

[29] C.L. Zhang, L.X. Zhao, Model-based neural network correlation for refrigerant mass flow rates through adiabatic capillary tubes, International Journal of Refrigeration 30 (2007) 690-698.

[30] Y. Islamoglu, A. Kurt, C. Parmaksizoglu, Performance prediction for non-adiabatic capillary tube suction line heat exchanger: an artificial neural network approach, Energy Conversion and Management 46 (2005) 223-232.

[31] R. Kumar, M.K. Khan, P.K. Sahoo, Flow characteristics of refrigerants flowing through capillary tubes – A review, Applied Thermal Engineering (2008) article in press doi:10.1016/j.applthermaleng.2008.08.020.

[32] B. Hallgren, H. Boterenbrood, H.J. Burckhart, H. Kvedalen, The Embedded Local Monitor Board (ELMB) in the LHC front-end I/O control system, Proceedings of the seventh workshop on electronics for LHC experiments, CERN Reports 2001 (5) (2001) 325-330.

[33] T.P. Brackbill, P.L. Young, S.G. Kandlikar, Estimating roughness parameters resulting from various machining techniques for fluid flow applications, Proceedings of 5th International Conference on Nanochannels, Microchannels and Minichannels (June 18-20, 2007), Puebla, Mexico, 827-836.

[34] V. Vacek, V. Vinš, A study of the flow through a capillary tube tuned up for the cooling circuit with fluoroinert refrigerants, International Journal of Thermophysics 28 (2007) 1490-1508.

[35] REFPROP version 7.0, Reference fluid thermodynamics and transport properties, NIST Standard Reference Database 23, Gaithersburg, MD 20899, USA, (2002).

ACCEPTED MANUSCRIPT

[36] V. Vacek, G. Hallewell, S. Lindsay, Velocity of sound measurements in gaseous per-fluorocarbons and their mixtures, Fluid Phase Equilibria 185 (2001) 305-314.

[37] V. Vacek, G. Hallewell, S. Ilie, S. Lindsay, Perfluorocarbons and their use in cooling systems for semiconductor particle detectors, Fluid Phase Equilibria 174 (2000) 191-201.

[38] MATLAB the language of technical computing, v. 6.5.0, The MathWorks, Inc. (2002).

[39] J.W. Ponton, J. Klemeš, Alternatives to neural networks for inferential measurement, Computers & Chemical Engineering 17 (1993) 991-1000.

[40] ASHRAE handbook: refrigeration / SI edition, chapter 45, ASHRAE, 1998, ISBN: 1883413540.

[41] S.J. Kuehl, V.W. Goldschmidt, Modeling of steady flows of R22 through capillary tubes, ASHRAE Transactions 97 (1991) 139-148.

ACCEPTED MANUSCRIPT

ACCEPTED MANUSCRIPT

FIGURE CAPTIONS:

Fig. 1. Scheme of the cooling circuit used for the capillary tube test

Fig. 2. Saturation pressure calculated from the experimentally measured temperature compared with results of the numerical model; R218; d = 0.548 mm; L = 1.3 m; T_{in} = 14.7°C; p_{in} = 8.5 bar; p_{evap} = 1.4 bar; $\dot{m} = 0.71$ g·s^{-1}

Fig. 3. Relative deviation of the mass flow rate of R218 correlated by the power law function

Fig. 4. Scheme of the three-layer perceptron with two neurons in the hidden layer

Fig. 5. Relative deviation of the mass flow rate of R218 correlated with the ANN – two neurons in the hidden layer

Fig. 6. Mass flow rate of R218 depending on the subcooled liquid temperature at the capillary tube inlet; comparison of the power law correlation, the ANN correlation and the experimental data

ACCEPTED MANUSCRIPT

ACCEPTED MANUSCRIPT

TABLES:

d [mm]	L [m]	ε/d [-]	min(m) [g·s^{-1}]	max(m) [g·s^{-1}]	min(p_{in}) [bar]	max(p_{in}) [bar]	min(T_{in}) [°C]	max(T_{in}) [°C]
0.474	0.700	0.004	0.55	0.88	7.3	10.4	15.8	20.1
0.530	0.440	0.004	1.83	2.22	12.9	13.0	-5.3	11.8
0.530	0.700	0.004	1.48	1.76	12.9	13.0	-9.9	10.4
0.530	0.895	0.004	1.41	1.51	12.9	13.0	-7.6	1.5
0.548	1.300	0.003	0.57	0.87	7.1	10.0	14.4	19.7
0.548	1.600	0.003	0.64	0.74	10.0	10.4	17.5	23.9
0.588	0.700	0.0025	1.94	2.50	13.2	13.5	-13.1	15.1
0.588	0.800	0.0025	2.20	2.29	13.2	13.4	-14.3	-2.0
0.588	0.900	0.0025	2.04	2.15	11.9	13.5	-14.7	-11.3
0.588	1.000	0.0025	2.00	2.09	13.2	13.3	-16.0	-5.5
0.797	2.261	0.003	1.88	2.92	10.9	13.0	-11.9	27.4
0.800	0.950	0.0025	4.78	4.95	12.9	13.5	-16.0	-14.0
0.800	1.050	0.003	4.50	4.75	13.4	13.4	-20.0	-9.0
0.800	1.250	0.003	4.11	4.30	12.6	13.3	-21.0	-18.0
0.800	1.500	0.003	3.02	3.90	13.0	13.1	-4.7	15.9
0.800	1.771	0.003	2.43	3.55	12.7	13.1	-13.0	20.2
0.802	0.398	0.0025	2.69	3.21	7.3	8.0	13.6	13.8
0.802	1.279	0.0025	1.70	2.40	7.5	10.0	13.3	15.6
0.985	6.510	0.002	1.77	2.99	10.1	14.2	-18.5	19.6
0.987	3.931	0.0015	1.59	2.96	8.1	13.1	-0.1	21.6
0.987	5.949	0.0015	1.72	2.54	10.9	14.4	21.8	23.5

Table 1. List of the tested capillary tubes and the ranges of refrigerant flow conditions

ACCEPTED MANUSCRIPT

ACCEPTED MANUSCRIPT

π-group	π_1	π_2	π_3	π_4	π_5	π_6	π_7
Parameter	$\frac{p_{in}-p_{sat}}{p_{crit}}$	$\frac{T_{in}-T_{cond}}{T_{crit}}$	$\frac{L}{d}$	$\frac{\rho_L}{\rho_V}$	$\frac{\mu_L-\mu_V}{\mu_V}$	$\frac{\sigma}{p_{in}d}$	$\frac{\rho_L\left(h_V-h_L\right)}{p_{sat}}$
Description	Inlet pressure	Subcooling	Geometry	Density	Friction	Bubble growth	Vaporization
π-group	π_8	π_9	π_{10}	π_{11}	π_{12}	π_{13}	
Parameter	$\frac{\dot{m}}{d^2\sqrt{\rho_L p_{in}}}$	$\frac{\dot{m}}{d\mu_L}$	$\frac{d^2\rho_L p_{in}}{\mu_L^2}$	$\frac{d^2\rho_L^2 c_{pL}\Delta T}{\mu_L^2}$	$\frac{d^2 h_{LV}}{v_L^2\mu_L^2}$	$\frac{d\rho_L\sigma}{\mu_L^2}$	
Description	Mass flow rate	Mass flow rate	Inlet pressure	Inlet condition	Vaporization	Bubble growth	

Table 2. Dimensionless parameters

ACCEPTED MANUSCRIPT

ACCEPTED MANUSCRIPT

π-group	min	max
π_1	0.011257	0.45502
π_2	0.020304	0.87511
π_3	496.26	6609.1
π_4	14.201	80.515
π_5	11.365	31.319
π_6	2.82E-06	1.30E-05
π_7	105.14	780.3
target π_8	0.046213	0.18084

Table 3. Minimum and maximum values of the π-parameters used for the data normalization

ACCEPTED MANUSCRIPT

ACCEPTED MANUSCRIPT

Correlation	Refrigerant / Data source	R12 [15,20,22]	R22 [15,16,18,23,24,41]	R134a [21,22]	R290 [24]	R600a [22]	R218 fitted data	R218 test data
Melo et al. [22]								
	AD	**-0.12**	6.48	**1.02**	-14.73	**1.24**	10.70	4.31
	SD	**4.09**	6.88	**7.18**	2.99	**4.89**	10.37	6.44
Kim et al. [23]								
	AD	-44.29	-1.96	-42.01	-34.55	-47.59	-28.14	-35.93
	SD	9.35	9.47	12.95	6.36	9.68	20.37	11.38
Choi et al. [24]								
	AD	5.28	14.09	-6.35	**2.47**	12.94	-10.91	-16.77
	SD	4.05	7.84	8.53	**2.83**	5.14	15.04	6.41
Choi et al. [25]								
	AD	0.86	15.56	-5.97	-0.02	10.29	-3.52	-11.61
	SD	5.89	9.34	9.80	4.42	6.24	19.63	6.69
Zhang [28]								
	AD	8.11	7.59	4.46	-13.16	12.68	-49.95	-1.92
	SD	6.78	8.43	7.78	1.94	7.89	79.65	12.31
ASHRAE [40]								
	AD	-16.07	**4.20**	-4.75	-23.44	-11.56	-42.59	-20.29
	SD	4.96	**7.91**	7.16	0.92	5.99	38.07	12.51
ANN (this work)	*AD*	-2.18	22.39	**-1.84**	1.89	**1.40**	**-0.12**	**-1.49**
	SD	7.24	8.91	**8.61**	5.05	**6.58**	**3.45**	**3.88**
Number of data points		24	84	20	6	19	189	34

Table 4. Average and standard deviations of the mass flow rate predicted by considered correlations both for the data presented in literature related to standard refrigerants and for our experimental data obtained with R218

ACCEPTED MANUSCRIPT

FIGURES:

Fig. 1

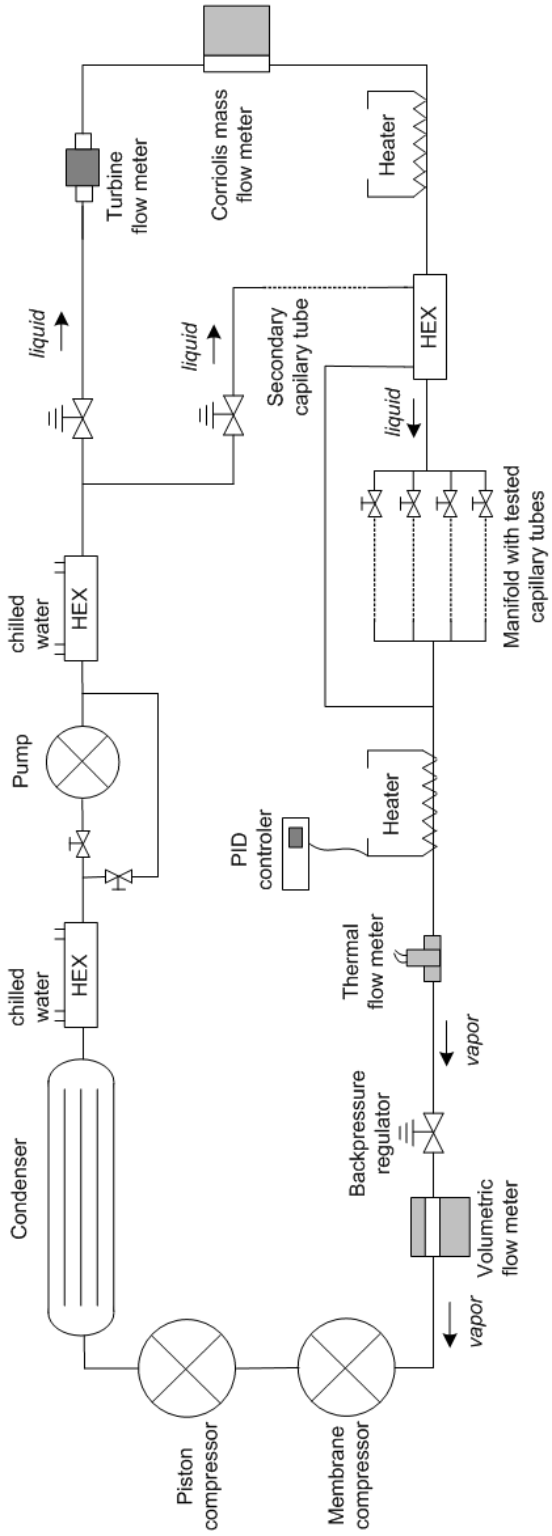

ACCEPTED MANUSCRIPT

Fig. 2

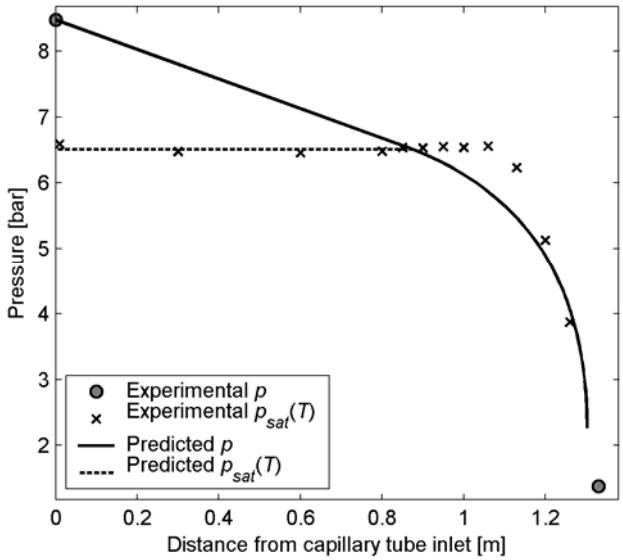

ACCEPTED MANUSCRIPT

ACCEPTED MANUSCRIPT

Fig. 3

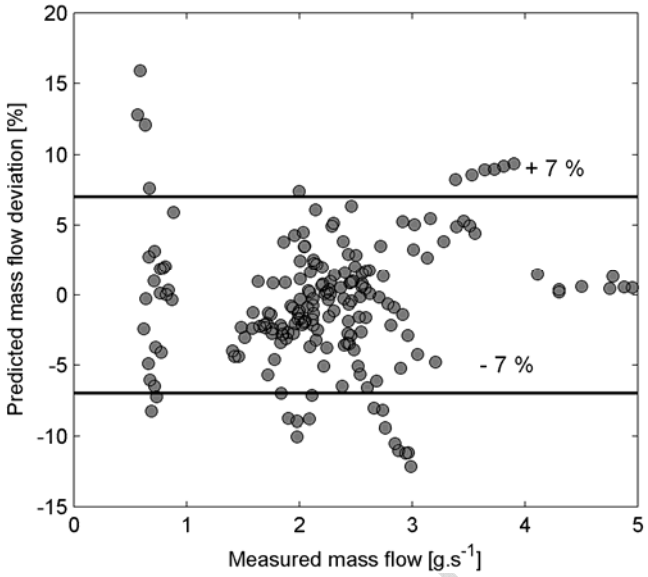

ACCEPTED MANUSCRIPT

ACCEPTED MANUSCRIPT

Fig. 4

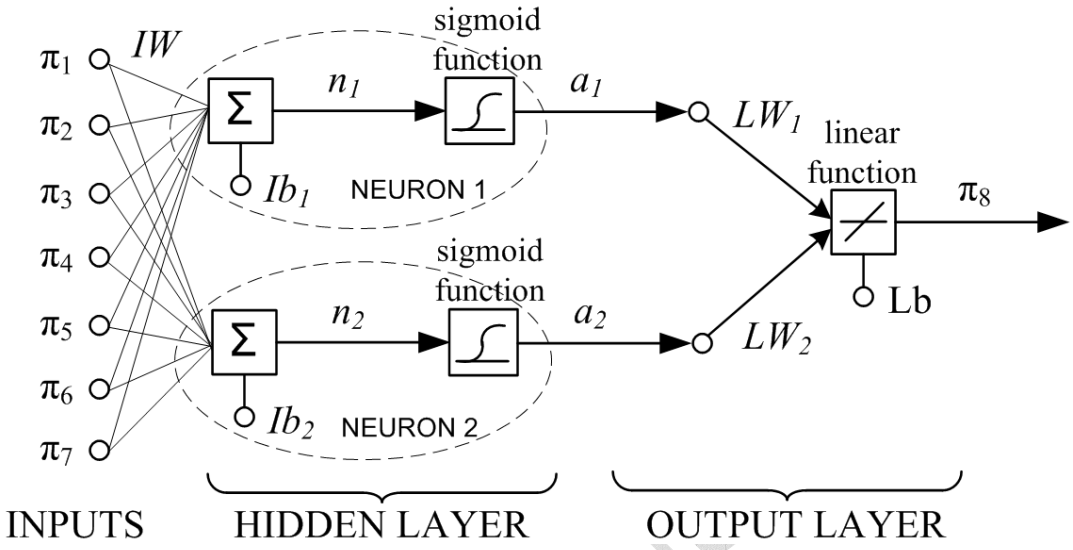

ACCEPTED MANUSCRIPT

ACCEPTED MANUSCRIPT

Fig. 5

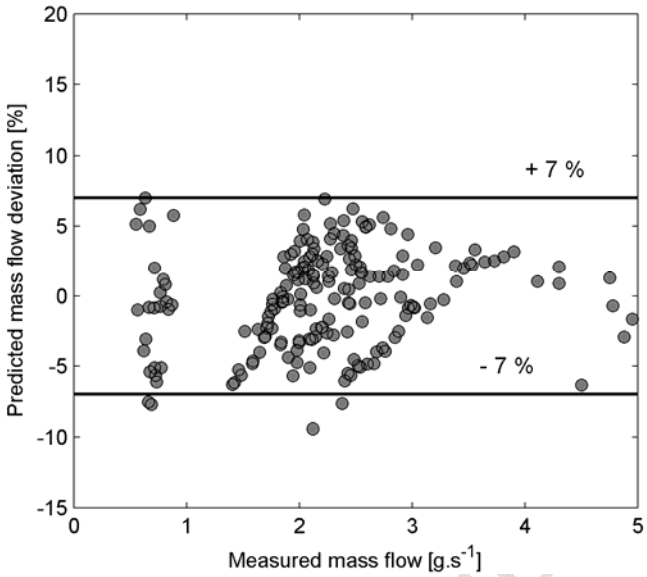

ACCEPTED MANUSCRIPT

Fig. 6

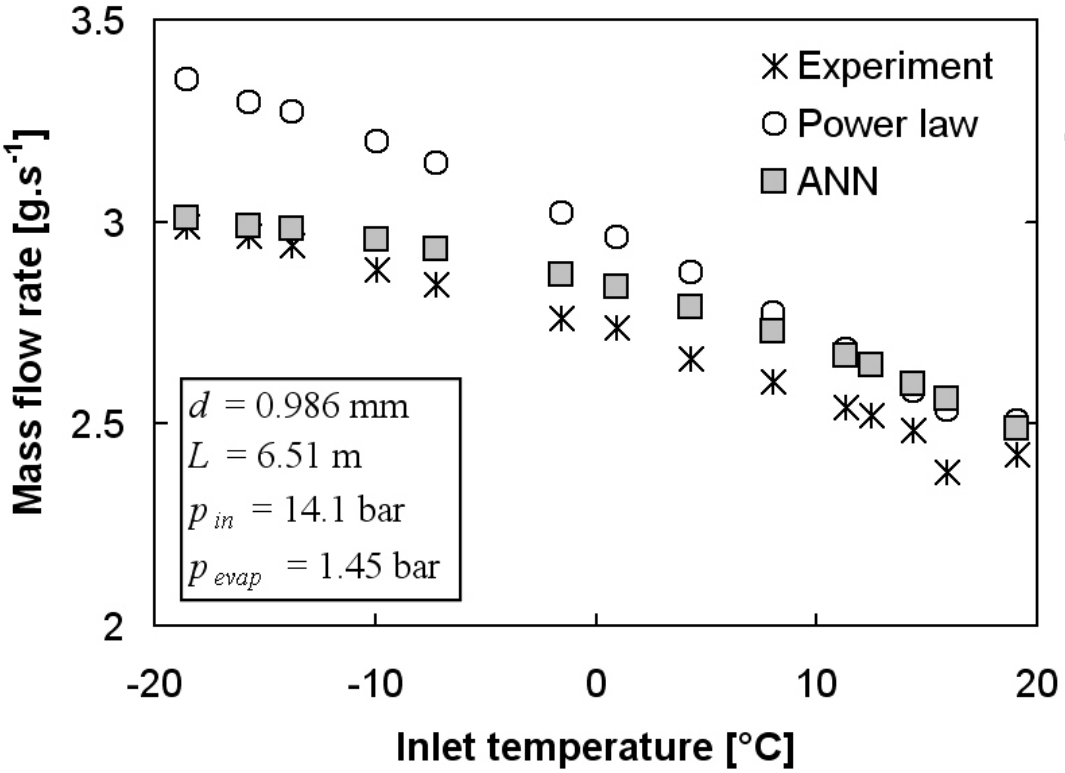

ACCEPTED